

## Research Article

# Detection of the Endosomal Sorting Complex Required for Transport in *Entamoeba histolytica* and Characterization of the EhVps4 Protein

Israel López-Reyes,<sup>1</sup> Guillermina García-Rivera,<sup>1</sup> Cecilia Bañuelos,<sup>1</sup> Silvia Herranz,<sup>2</sup> Olivier Vincent,<sup>2</sup> César López-Camarillo,<sup>3</sup> Laurence A. Marchat,<sup>4</sup> and Esther Orozco<sup>1</sup>

<sup>1</sup>Departamento de Infectómica y Patogénesis Molecular, Centro de Investigación y de Estudios Avanzados del IPN, México, CP 07360, Mexico

<sup>2</sup>Departamento de Modelos Experimentales de Enfermedades Humanas, Instituto de Investigaciones Biomédicas CSIC-UAM, Madrid, CP 28029, Spain

<sup>3</sup>Universidad Autónoma de la Ciudad de México, Posgrado en Ciencias Genómicas, México, CP 03100, Mexico

<sup>4</sup>Escuela Nacional de Medicina y Homeopatía del IPN, Programa Institucional de Biomedicina Molecular, México, CP 07320, Mexico

Correspondence should be addressed to Esther Orozco, orozco.esther@gmail.com

Received 23 September 2009; Revised 1 March 2010; Accepted 1 March 2010

Academic Editor: Abhay R. Satoskar

Copyright © 2010 Israel López-Reyes et al. This is an open access article distributed under the Creative Commons Attribution License, which permits unrestricted use, distribution, and reproduction in any medium, provided the original work is properly cited.

Eukaryotic endocytosis involves multivesicular bodies formation, which is driven by endosomal sorting complexes required for transport (ESCRT). Here, we showed the presence and expression of homologous ESCRT genes in *Entamoeba histolytica*. We cloned and expressed the *EhVps4* gene, an ESCRT member, to obtain the recombinant EhVps4 and generate specific antibodies, which immunodetected EhVps4 in cytoplasm of trophozoites. Bioinformatics and biochemical studies evidenced that rEhVps4 is an ATPase, whose activity depends on the conserved E211 residue. Next, we generated trophozoites overexpressing EhVps4 and mutant EhVps4-E211Q FLAG-tagged proteins. The EhVps4-FLAG was located in cytosol and at plasma membrane, whereas the EhVps4-E211Q-FLAG was detected as abundant cytoplasmic dots in trophozoites. Erythrophagocytosis, cytopathic activity, and hepatic damage in hamsters were not improved in trophozoites overexpressing EhVps4-FLAG. In contrast, EhVps4-E211Q-FLAG protein overexpression impaired these properties. The localization of EhVps4-FLAG around ingested erythrocytes, together with our previous results, strengthens the role for EhVps4 in *E. histolytica* phagocytosis and virulence.

## 1. Introduction

*Entamoeba histolytica* is the enteric protozoan parasite responsible for human amoebiasis that affects 50 million people around the world, causing colitis and liver abscesses [1]. In this organism, phagocytosis and vesicular trafficking play a critical role in ingestion and degradation of host cells and microorganisms. Vacuolar protein sorting (Vps) factors and some proteins that participate in vesicle transport in eukaryotes have been identified in *E. histolytica* [2–4].

In eukaryotic cells, endocytosis consists in phagocytosis, micropinocytosis and pinocytosis. Particularly, phagocytosis involves the ingestion of particles of varying size into

phagosomes, which sequentially fuse with early and late endosomes forming multivesicular bodies (MVB), as well as with lysosomes to form phagolysosomes [5]. Additionally, MVB are critical for cell receptors down-regulation, retroviral budding and other processes [6–8]. MVB formation is driven by the assembly of endosomal sorting complexes required for transport (ESCRT), which result from the interaction of different class E Vps proteins [9, 10].

The MVB-sorting process initiates with the association of Vps27 and Hse1 proteins to form the ESCRT-0 complex, which is targeted to endosomal membrane domains that bind ubiquitinated cargo proteins (reviewed in [6, 7]). Then, ESCRT-0 recruits ESCRT-I formed by Vps23, Vps28, and

Vps37 proteins, as well as an additional subunit called Mvb12 [11, 12]. Later, ESCRT-II, composed by Vps22, Vps25, and Vps36 proteins, is activated by ESCRT-I [13]. Ubiquitinated cargo proteins are recognized by ESCRT-I via Vps23 and by ESCRT-II via Vps36. Then, ESCRT-III, formed by Vps20, Vps32, Vps2, and Vps24, interacts with ESCRT-II components to complete ESCRT formation [14]. ESCRT-III is required for cargo molecules concentration into MVB vesicles and it coordinates the association of Bro1 protein and Doa4-deubiquitinating enzyme [15–17]. Finally, Vps4 protein catalyzes the ATP-dependent dissociation of ESCRT complexes from endosomes to initiate new rounds of vesicle formation and cargo molecules transport [6, 7]. Particularly, it has been reported that substitution of the conserved E amino acid residue by a Q residue in the Vps4 ATPase motif impairs ATP hydrolysis activity [18, 19], resulting in an inefficient protein transport from endosomal compartments to vacuoles or lysosomes [20–22], which evidenced the critical role of Vps4 in protein transport and vesicle trafficking.

In *E. histolytica*, experimental evidence suggests that MVB-like structures are formed by fusion of inward budding membranes with phagosomes [23]. Ubiquitin, deubiquitinating enzymes and a SNF7 homologue (vesicular trafficking protein) have been identified in isolated phagosomes by proteomic analysis, suggesting that a mechanism similar to MVB formation could be present in *E. histolytica* [23–25]. Additionally, the Bro1 domain-containing EhADH112 protein, which forms part of the *E. histolytica* EhCPADH complex involved in parasite virulence, is located in MVB-like structures in trophozoites [26, 27]. However, molecular mechanisms regulating MVB formation in *E. histolytica* remain poorly understood. Here, by *in silico* analysis from parasite genome databases, we identified 20 ESCRT protein-encoding genes in *E. histolytica* and showed that most of them were transcribed in trophozoites. Since Vps4 has been described as a key molecule to complete the disassembly of ESCRT and associated factors in other systems, we initiated the study of ESCRT machinery in *E. histolytica* by cloning and characterizing the EhVps4 protein. Biochemical assays showed that EhVps4 exhibits ATPase activity *in vitro*. Interestingly, by using trophozoites overexpressing the wild type and a mutant version of EhVps4, we provide data supporting a role for this protein in phagocytosis and virulence.

## 2. Material and Methods

**2.1. In Silico Identification of Putative ESCRT Genes in *E. histolytica*.** Sequence similarity searches for ESCRT genes were performed in *E. histolytica* genome database (<http://pathema.jcvi.org/cgi-bin/Entamoeba/PathemaHomePage.cgi>) by BLAST using human and yeast ESCRT protein sequences as queries. Putative *E. histolytica* ESCRT homologous proteins were selected using the following criteria: (i) at least 20% identity and 35% similarity to the query sequence; (ii) *e*-value lower than 0.002; and (iii) absence of stop codons in the coding sequence. Predicted

amino acids sequences were aligned by ClustalW software (<http://www.ebi.ac.uk/clustalw/>). Functional and structural domains were predicted using PROSITE (<http://www.expasy.org/tools/scanPROSITE/>) and Pfam (<http://www.sanger.ac.uk/Software/Pfam/>) databases. Phylo-genetic relationships among putative ESCRT proteins from *E. histolytica* and other organisms were analyzed using the Neighbor-Joining distance method [28] as implemented in the MEGA package version 3.1 [29]. Phylogenetic trees were generated for each putative *E. histolytica* ESCRT protein aligned with homologues from different species. Robustness of phylogenetic inferences was tested by bootstrapping method, involving 1000 replications of the data based on the criteria of 50% majority-rule consensus.

For 3D modeling of MIT and AAA domains of *E. histolytica* EhVps4, predicted tertiary structures were obtained with the Phyre server (<http://www.sbg.bio.ic.ac.uk/phyre/>), using crystal data from yeast Vps4 MIT (2v6xA) and AAA (2qpaB) domains as templates.

**2.2. *E. histolytica* Cultures.** Trophozoites of *E. histolytica* clone A (strain HM1: IMSS) were axenically cultured in TYI-S-33 medium at 37°C and harvested during exponential growth phase [30]. Medium for transfected trophozoites was supplemented with 40 µg/mL G418 (Gibco). Cell viability was monitored by microscopy using Trypan blue dye exclusion test.

**2.3. Semi-Quantitative RT-PCR Assays.** Using Trizol reagent (Invitrogen), total RNA was extracted from 10<sup>6</sup> trophozoites grown in TYI-S-33 medium or 5 minutes after red blood cells (RBC) ingestion. Semiquantitative RT-PCR was performed using 1 µg of DNase I-treated total RNA that was reverse transcribed using Superscript II (Invitrogen) for 2 hours at 42°C. Control samples without Superscript-II were included in all experiments. cDNA samples were subjected to PCR amplification using specific internal primers for distinct *E. histolytica* putative ESCRT genes (see Table T1 in Supplementary material available on line at doi: 10.1155/2010/890674). Briefly, PCR consisted in an initial denaturation step at 94°C for 5 minutes followed by 25 cycles of 35 s at 94°C, 30 s at T<sub>m</sub> calculated for each gene (Supplementary data Table T1), 1 minute 30 s at 72°C and a final extension step at 72°C for 7 minutes. As a control, we amplified a *Eh25S rRNA* gene internal sequence which was used to normalize densitometric data. Products were separated by 1% agarose gel electrophoresis, stained with ethidium bromide and visualized by UV light in a Gel Doc 1000 apparatus (BioRad). Densitometric analysis was performed using the Quantity One software. Three independent experiments were done by duplicate. Statistical significance was determined by *T* Student test [31].

**2.4. Cloning and Sequencing of *EhVps4* and *EhVps4-E211Q* Genes.** The full-length *EhVps4* gene (1260 bp) reported at locus EHI\_118900 in *E. histolytica* Pathema database was PCR amplified from *E. histolytica* genomic DNA using the

*EhVps4*-forward (5'-CCCCGGATCCATGACATCGTTACTTGATAAAGG-3') and *EhVps4*-reverse (5'-CCCCCTCGAGTTATCCATCTTGTCCAAATTGTTC-3') primers in the presence of 0.2 U Pfx DNA polymerase (Invitrogen). Briefly, PCR consisted in an initial denaturation step at 94°C for 5 minutes followed by 28 cycles (30 s at 94°C, 35 s at 55°C, and 1 minute 30 s at 72°C) and a final extension step at 72°C for 7 minutes. The PCR product was cloned into TOPO vector (Invitrogen) yielding the TOPO-*EhVps4* plasmid. Using the QuikChange mutagenesis kit (Stratagene), we generated a point mutation in the EhVps4 ATPase domain at amino acid 211 to replace glutamic acid (E) by glutamine (Q) to obtain the TOPO *EhVps4*-E211Q plasmid. Both constructions were confirmed by automated DNA sequencing. Then, *EhVps4* and *EhVps4*-E211Q genes were PCR amplified from TOPO plasmids and subcloned in the pGEX-6P1 expression vector (Amersham Biosciences) to generate the recombinant pGEX-6P1-*EhVps4* and pGEX-6P1-*EhVps4*-E211Q plasmids, respectively. Constructions were confirmed by automated DNA sequencing.

**2.5. Expression and Purification of Recombinant EhVps4-GST and EhVps4-E211Q-GST Proteins.** *Escherichia coli* BL21 (DE3) pLysS (Invitrogen) bacteria were transformed with pGEX-6P1-*EhVps4* or pGEX-6P1-*EhVps4*-E211Q plasmids to produce the GST-tagged rEhVps4 and rEhVps4E211Q proteins. Bacteria were grown at 37°C in 2-TY medium containing 100 µg/mL ampicillin and 34 µg/mL chloramphenicol. rEhVps4-GST expression was induced by 1 mM isopropyl beta-D-thiogalactopyranoside (IPTG) for 3 hours at 37°C. Cells were harvested, resuspended in ice cold PBS buffer (140 mM NaCl, 2.7 mM KCl, 10 mM Na<sub>2</sub>HPO<sub>4</sub>, and 1.8 mM KH<sub>2</sub>PO<sub>4</sub> pH 7.3) and lysed by sonication at 4°C in the presence of lysozyme (1 mg/mL). rEhVps4-GST and rEhVps4-E211Q-GST polypeptides were purified near to homogeneity through glutathione affinity chromatography, according to manufacturer recommendations (Amersham Biosciences). To further use the recombinant protein as antigen, the GST tag (25 kDa) was removed from rEhVps4-GST protein by incubation with 2 U PreScission Protease (Amersham Biosciences) during 12 hours at 4°C. Cleaved rEhVps4 protein was dialyzed into PBS pH 7.4. Identity and integrity of purified rEhVps4-GST, rEhVps4-E211Q-GST and rEhVps4 proteins were confirmed by 10% SDS-PAGE and Western blot assays using anti-GST, (GE-Healthcare, 1 : 5000 dilution) and anti-rEhVps4 (1 : 15000 dilution) antibodies, respectively, and the ECL-Plus Western blotting detection system (Amersham Biosciences).

**2.6. Generation of Polyclonal Antibodies against EhVps4.** Purified rEhVps4 without GST tag was submitted to preparative 10% SDS-PAGE and electroeluted from Coomassie stained gels. rEhVps4 (200 µg) in complete Freund's adjuvant (Sigma) was subcutaneously inoculated into a New Zealand male rabbit, and then, three doses of 100 µg rEhVps4 in incomplete Freund's adjuvant were injected at 15 days intervals. Rabbit was bled to obtain polyclonal serum.

**2.7. ATPase Activity Assay.** The ATPase activity assay procedure was based on that previously described [32] using the PiPer Phosphate Assay kit (Invitrogen), with minimal modifications. Briefly, Amplex red was diluted in DMSO to a 10 mM final concentration. Maltose phosphorylase, maltose, glucose oxidase, and horseradish peroxidase were diluted in enzyme buffer (0.1 M Tris-HCl, pH 7.5) to a final concentration of 200 U/mL, 40 mM, 200 U/mL, and 100 U/mL, respectively. Assay buffer (100 mM Tris, 20 mM KCl, and 6 mM MgCl<sub>2</sub>, pH 7.4) was added to a 96-well plate. The volume corresponding to 3.5 µg and 5 µg of purified and dialyzed rEhVps4-GST, rEhVps4-E211Q-GST, and rGST proteins was added to wells and enzyme buffer was added up to 27 µL. 50 µL of working solution (2 U/mL glucose oxidase, 4 U/mL maltose phosphorylase, 0.4 mM maltose, 100 µM amplex red, 0.4 U/mL HRP) were added to wells. Controls consisting in enzyme buffer or enzyme buffer with working solution were included. Fresh ATP was diluted in assay buffer to a concentration of 2.5 mM and added to each well to a final volume of 100 µL. Plates were mixed by pipetting and shaken for 30 s to ensure homogeneity. Then, reactions were kept at 25°C for 30 minutes and protected from the light. The absorbance was measured at 562 nm at 30 minutes and data were documented. The purified rGST protein was used as negative control in ATPase assays. Assays were performed twice by triplicate.

**2.8. Plasmids Construction for Transfection Assays.** The mutant *EhVps4*-E211Q gene and the wild type *EhVps4* gene were PCR amplified from TOPO *EhVps4*-E211Q and TOPO-*EhVps4*, respectively, using the *EhVps4*-S-*KpnI* (5'-CCCCGGTACCATGACATCGTTACTTGATAAAGG-3') and *EhVps4*-AS-FLAG-*BamHI* (5'-CCCCGGATCCTTACTTATCGTCGTCATCCTTGTAATCTCCATCTTGTCCAAATTGTTC-3') primers and cloned into pNEO vector for further transfection assays [33]. The underlined nucleotide sequence corresponds to the FLAG epitope (1 kDa) [34] that was added to the carboxy terminus of recombinant proteins to allow their specific immunodetection in transfected trophozoites. The resulting plasmids named p*EhVps4*-E211Q and p*EhVps4* were confirmed by automated DNA sequencing.

**2.9. In Vitro and In Vivo Virulence of Transfected Cells.** Trophozoites were transfected with 200 µg of p*EhVps4*-E211Q, p*EhVps4* and control pNEO plasmids by electroporation as described [33]. Briefly, amoebae (10<sup>7</sup>) were washed twice in cold PBS and once in cold complete cytomix buffer. Electroporation was performed with the Bio-Rad Gene Pulser using 1200 V/cm and 25 µF, with a constant time of 0.4 ms. Electroporated cells were transferred into fresh culture medium for 48 hours before selecting them with 10 µg/mL G418.

In vitro virulence of nontransfected and transfected trophozoites (10<sup>5</sup>) was measured on MDCK cells (6 × 10<sup>4</sup>) as described [35, 36]. Rate of erythrophagocytosis was evaluated using trophozoites and RBC in a 1 : 100 relation, at 5, 10, and 15 minutes [37].

In vivo virulence of transfected trophozoites was evaluated as described [38]. Briefly, under sterile conditions and intraperitoneal anaesthesia with 0.2 mg Anesthasal (Pfizer), three groups of six hamsters each were laparotomized and intraperitoneally challenged with p*EhVps4*-E211Q, p*EhVps4*, or p*NEO* transfected trophozoites ( $2.5 \times 10^6$ ) in a volume of 0.1 mL PBS using a 29-gauge needle. Seven days after challenge, animals were anaesthetized and livers were removed to evaluate hepatic damage.

**2.10. Immunodetection of *EhVps4* in Trophozoites.** Western blot assays were performed using 30  $\mu$ g of total proteins from nontransfected or p*NEO*, p*EhVps4*, and p*EhVps4*-E211Q transfected trophozoites. We used anti-FLAG monoclonal (1 : 700) or anti-r*EhVps4* polyclonal (1 : 15000) antibodies and rabbit anti-mouse and goat anti-rabbit IgG horseradish peroxidase-labeled secondary antibodies (Zymed; 1 : 10000), respectively. Immunodetected proteins were revealed with the ECL Plus Western blotting system (Amersham Biosciences). As an internal control, we used monoclonal antibodies raised against *E. histolytica* actin (1 : 1000) and goat anti-mouse IgG horseradish peroxidase-labeled secondary antibodies (Zymed; 1 : 10000).

For confocal microscopy assays, nontransfected and transfected trophozoites were grown on coverslips, fixed with 4% paraformaldehyde at 37°C for 1 hour, permeabilized with Triton X-100 and blocked with 1% bovine serum albumin in PBS. Then, nontransfected and transfected cells were incubated with polyclonal anti-r*EhVps4* (1 : 5000) or monoclonal anti-FLAG primary antibodies (Sigma; 1 : 500), respectively, at 37°C for 2 hours, followed by incubation with anti-rabbit or anti-mouse fluoresceinated (Zymed; 1 : 100) monoclonal antibodies, at 37°C for 1 hour. Next, trophozoites were washed three times with PBS 1X at room temperature and DNA was counterstained with 4',6-diamidino-2-phenylindole (DAPI) (5  $\mu$ g/mL) for 5 minutes. To immunolocalize *EhVps4* during erythrophagocytosis, p*EhVps4* transfected cells were incubated with RBC (1 : 20) for 10 minutes. Ingested RBC were stained with diaminobenzidine (0.84 mM 3,3'-diaminobenzidine, 0.048% H<sub>2</sub>O<sub>2</sub> and 50 mM Tris-HCl, pH 9.5) for 5 minutes and cells were incubated with polyclonal anti-r*EhVps4* (1 : 5000) to be processed for immunofluorescence as described above. Light optical sections (1.5  $\mu$ m) were obtained through a Leica inverted microscope attached to a laser confocal scanning system TCS-SP2 (Leica).

### 3. Results

**3.1. *E. histolytica* Genome Contains Homologous ESCRT Genes That Are Expressed in Trophozoites.** To investigate the presence of ESCRT-related genes in *E. histolytica*, we surveyed the parasite genome sequence at Pathema database using the amino acid sequences of yeast and human ESCRT proteins as queries. We detected a set of 20 putative ESCRT protein-encoding genes, which exhibited significant *e*-values ( $1.1e - 114$  to 0.00032) and high similarity (20 to 62%) to yeast and human ESCRT (ESCRT 0-III and associated factors) orthologues (see Table 1). However, we

did not find homologues for yeast Mvb12, and Bullp protein involved in protein ubiquitination, neither human Vps37-B and Vps37-C proteins. Phylogenetic inference revealed that *E. histolytica* ESCRT predicted proteins are closely related to homologous proteins from other protozoa, such as *Giardia lamblia*, *Tetrahymena thermophila*, *Trichomonas vaginalis*, *Plasmodium vivax*, *Cryptosporidium homini*, and *Trypanosoma cruzi* (data not shown). Bioinformatics analysis showed that *E. histolytica* ESCRT predicted proteins have the most characteristic functional domains (see Supplementary data Figure S1) and tertiary structure folding described for yeast and human ESCRT factors (data not shown).

To determine whether the putative *E. histolytica* ESCRT genes were expressed, we performed RT-PCR assays for the 16 most conserved genes. In basal culture conditions, 15 genes were transcribed, but the *EhVps22* transcript was not detected in these experiments (see Figures 1(a) and 1(b)). We also performed RT-PCR assays using RNA obtained from trophozoites incubated with RBC for 5 minutes to investigate whether erythrophagocytosis has an effect on ESCRT gene expression (see Figures 1(a) and 1(b)). In these assays, we found that all genes were expressed during erythrophagocytosis at similar levels as in basal conditions. Again, we did not detect the *EhVps22* gene expression. Interestingly, *EhVps23* and *Ehadh112* were 2- and 3-fold up-regulated, respectively. By densitometric analysis, the band given by the amplified *Eh25S rRNA* product in both conditions was taken as 100% and used to normalize ESCRT genes data.

**3.2. The Predicted *EhVps4* Protein Conserves the Typical Architecture of *Vps4* Homologues.** Since *Vps4* orthologues have been described as key molecules for the dissociation of ESCRT, we first focused on the characterization of the *E. histolytica* *EhVps4* protein. The predicted *EhVps4* contains the N-terminal MIT (microtubule interacting and transport), AAA (ATPase associated with a variety of activities) and *Vps4* C-terminal domains (see Figure 2(a)) that are characteristic and essential for *Vps4* proteins biological functions [39, 40]. Phylogenetic trees revealed that *EhVps4* is more related to protozoan *Vps4* than orthologous proteins from higher eukaryotes (see Figure 2(b)). Interestingly, 3D modeling of *EhVps4*, using the crystal structure of MIT and AAA domains from yeast *Vps4p* and human *Vps4B* as templates (see Figure 2(c)), showed that *EhVps4* region spanning the N-terminal MIT and AAA ATPase domains exhibited a similar folding with the conserved *Vps4*  $\alpha$ -helices.

**3.3. Expression and Immunodetection of *EhVps4* Protein in Trophozoites.** We produced and purified the recombinant *EhVps4* protein as a GST-tagged fusion polypeptide (r*EhVps4*-GST) in *E. coli* (see Figure 3(a), lanes 3, 4). By Western blot assays using commercial anti-GST monoclonal antibodies, we immunodetected the purified r*EhVps4*-GST as a 72 kDa protein in IPTG-induced bacteria (see Figure 3(b), lane 2) but not in protein extracts from noninduced bacteria (see Figure 3(b), lane 1). The r*EhVps4*-GST was digested with the PreScission Protease to obtain the r*EhVps4*

TABLE 1: Comparison of *Entamoeba histolytica*, *Homo sapiens*, and *Saccharomyces cerevisiae* ESCRT machineries.

Putative complex	Predicted protein	<i>Entamoeba histolytica</i>					<i>Homo sapiens</i>					<i>Saccharomyces cerevisiae</i>						
		Accession number <sup>a</sup>	Protein	Accession number <sup>b</sup>	e-value	S (%)	I (%)	Protein	Accession number <sup>a</sup>	e-value	S (%)	I (%)	Protein	Accession number <sup>a</sup>	e-value	S (%)	I (%)	
ESCRT-0 complex	EhHse1	EHL_091530	STAM1	Q92783	9e-08	72	50	Hse1p	P38753	2e-10	70	62						
	EhVps27	EHL_117910	HRS	O14964	—	—	—	Vps27p	P40343	1e-11	61	49						
	EhVps23	EHL_135460	TSG101	Q99816	1.4e-10	51	33	Vps23p	P25604	0.0052	31	25						
ESCRT-I complex	EhVps28	EHL_108630	hVps28	Q9UK41	—	—	—	Vps28p	Q02767	0.00057	45	28						
	EhVps37A	EHL_077870	hVps37A	Q6NWX7	0.00022	55	24	Vps37p	Q99176	0.00084	46	21						
	EhVps37D	EHL_060400	hVps37D	Q6P2C3	3.8e-06	50	35	nd	—	—	—	—						
	nd	—	nd	—	—	—	—	Mvb12	P42939	—	—	—						
ESCRT-II complex	EhVps22	EHL_131120	EAP30	Q96H20	9e-22	47	30	Vps22p	Q12483	3.4e-15	48	25						
	EhVps25	EHL_137860	EAP20	Q9BRG1	9e-08	52	28	Vps25p	P47142	0.00038	46	19						
	EhVps36	EHL_045320	EAP45	Q86VN1	1.8e-15	49	25	Vps36p	Q06696	1.1e-09	48	26						
ESCRT-III complex	EhVps2	EHL_194400	CHMP2A	O43633	8.9e-24	55	29	Vps2p	P36108	2e-05	50	29						
	EhVps20	EHL_066730	CHMP2B	Q9UQN3	7.9e-16	48	25	—	—	—	—	—						
	EhVps24	EHL_048690	CHMP6	Q96FZ7	—	—	—	Vps20p	Q04272	0.00015	54	26						
	EhVps32	EHL_169820	CHMP3	Q9Y3E7	—	—	—	Vps24p	P36095	2.2e-05	48	22						
		—	—	CHMP4A	Q9BY43	0.0012	48	24	Vps32p	P39929	2.5e-12	48	25					
Vps4	EhVps4	EHL_118900	CHMP4B	Q9H444	9.6e-07	43	20	nd	—	—	—	—						
	—	—	CHMP4C	Q96CF2	1.4e-06	43	20	nd	—	—	—	—						
Other MVB proteins	EhVta1	EHL_010040	hVps4A	Q9UN37	1.1e-114	69	52	Vps4p	P52917	3e-114	78	60						
	EhVps46	EHL_093850	hVps4B	O75351	3e-114	78	60	—	—	—	—	—						
	EhDoa4	EHL_012290	hVta1	Q9NP79	2.8e-05	44	23	Vta1p	Q06263	—	—	—						
Ubiquitination components	EhADH112	EHL_181220	CHMP1A	Q9HD42	—	—	—	Vps46p	P69771	0.00032	48	18						
	nd	—	CHMP1B	Q7LBR1	—	—	—	nd	—	—	—	—						
	EhRsp5	EHL_011530	CHMP5	Q9NZZ3	5.6e-15	45	28	Vps60p	Q03390	9e-06	46	19						
	—	—	UBP4	Q13107	1e-77	58	36	Doa4p	P32571	2e-27	50	31						
Ubiquitination components	nd	—	ALIX	Q9UKL5	1e-21	40	20	Rim20p	Q12033	2e-12	38	21						
	EhRsp5	EHL_011530	NEED4	P46934	1.6e-50	53	33	BRO1p	P48582	0.003	50	32						
Ubiquitination components	EhRsp5	EHL_011530	NEED4	P46934	1.6e-50	53	33	Bullp	P48524	—	—	—						
Ubiquitination components	EhRsp5	EHL_011530	NEED4	P46934	1.6e-50	53	33	Rsp5p	P39940	7.8e-57	57	36						

<sup>a</sup>Pathema Entamoeba Bioinformatics Resource Center. <sup>b</sup>Swiss-Prot/TrEMBL databases. nd: not determined. —: Denote nonsignificant similarity/identity and e-values. S: Similarity. I: Identity.

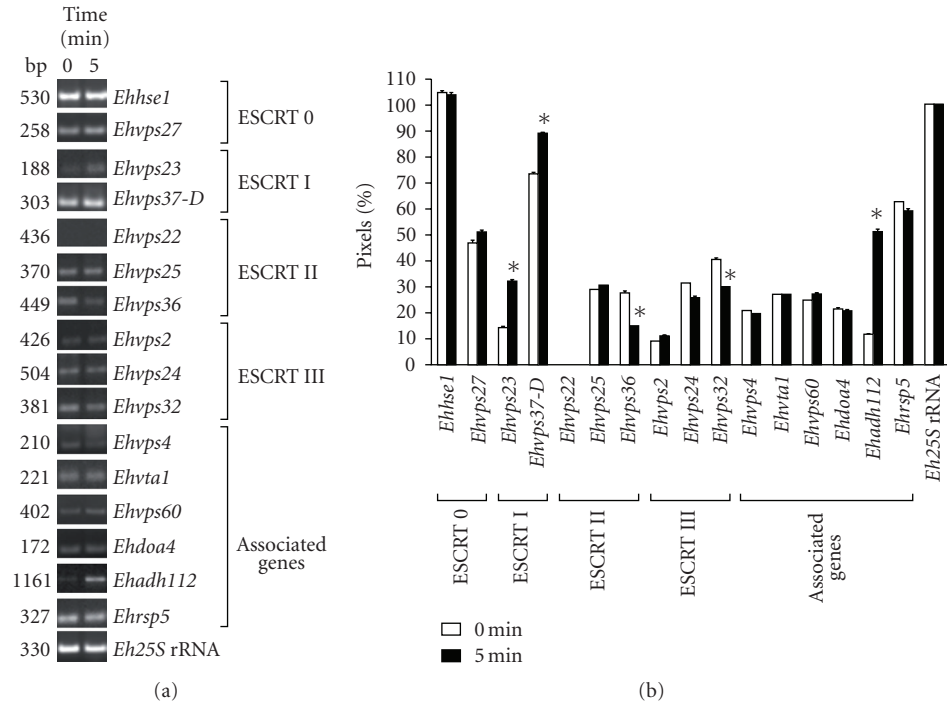


FIGURE 1: mRNA expression profile of *E. histolytica* putative ESCRT machinery genes. (a) RT-PCR products obtained from 1  $\mu$ g of total RNA from trophozoites growing in TYI-S-33 medium (0 minute) or after 5 minutes of erythrophagocytosis. (b) Densitometric analysis of RT-PCR products in (a). Pixels corresponding to *Eh25S rRNA* amplified product were taken as 100% in each lane. Data represent the mean of three independent experiments performed by duplicate for each gene. Asterisk, genes whose transcription is significantly changed according to *T* Student test.

untagged protein (47 kDa) (see Figure 3(c), lanes 2 and 3), which was also purified (see Figure 3(c), lane 4) and used to generate rabbit polyclonal antibodies. Anti-rEhVps4 serum recognized the untagged rEhVps4 protein, confirming the antibodies specificity (see Figure 3(d)). In addition, the same antibodies detected a single 47 kDa band in *E. histolytica* protein extracts (see Figure 3(e), lane 1), which corresponds to the expected molecular weight for the predicted EhVps4 polypeptide amino acid sequence. Antibodies did not detect any other AAA ATPases predicted in the *E. histolytica* genome [41]. Pre-immune serum, used as a control, did not recognize any band in trophozoite extracts (see Figure 3(e), lane 2). Through immunofluorescence and laser confocal microscopy assays, the specific rabbit polyclonal antibodies revealed EhVps4 as abundant small dots dispersed in the cytosol (see Figure 3(f)).

**3.4. ATPase Activity Assays.** To investigate whether the recombinant protein exhibited ATPase activity we used the rEhVps4 purified protein and a mutant version (EhVps4-E211Q) in which we changed the E211 residue of the AAA motif, essential for enzyme activity, by a Q residue (see Figure 4(a)) [18, 42]. Reactions were carried out using the PiPer Phosphate Assay Kit (Invitrogen) in the presence of 500  $\mu$ M ATP. Inorganic phosphate (Pi) release was measured spectrophotometrically at  $A_{562}$ . At zero time, absorbance values of samples containing rEhVps4-GST, rEhVps4-E211Q-GST and control rGST purified proteins (see Figure 4(b)) were

similar and they were taken as background. At 30 minutes,  $A_{562}$  values increased to  $0.115 \pm 0.008$  and  $0.162 \pm 0.022$ , using 3.5  $\mu$ g and 5  $\mu$ g of rEhVps4-GST protein, respectively. No significant  $A_{562}$  increase was detected when we used rEhVps4-E211Q-GST or rGST proteins at 30 minutes (see Figure 4(c)). These results showed that rEhVps4-GST has ATPase activity and that the AAA motif is essential for ATP hydrolysis.

**3.5. Generation of Trophozoites Overexpressing the EhVps4-FLAG and Mutant EhVps4-E211Q-FLAG Proteins.** To investigate the role of EhVps4 in *E. histolytica*, we generated transfectant trophozoites that overexpress the EhVps4 and the mutant EhVps4-E211Q FLAG-tagged proteins (see Figure 5(a)). Trophozoites transfected with pNEO vector were used as control in these experiments. Viability of transfected trophozoites was up to 90% as determined by trypan blue exclusion assays.

RT-PCR assays, using specific primers for *Ehvps4* gene, showed that trophozoites transfected with p*Ehvps4* or p*Ehvps4*-E211Q plasmids expressed a higher amount of the *Ehvps4* transcript in comparison to pNEO transfected cells (see Figure 5(b), upper panel, lanes 1, 2, and 3). As control, we amplified the *Eh25S rRNA* transcript, which showed minimal changes among the different transfectants studied (see Figure 5(b), lower panel).

By Western blot assays, using the anti-FLAG antibodies, we detected the EhVps4-FLAG and EhVps4-E211Q-FLAG

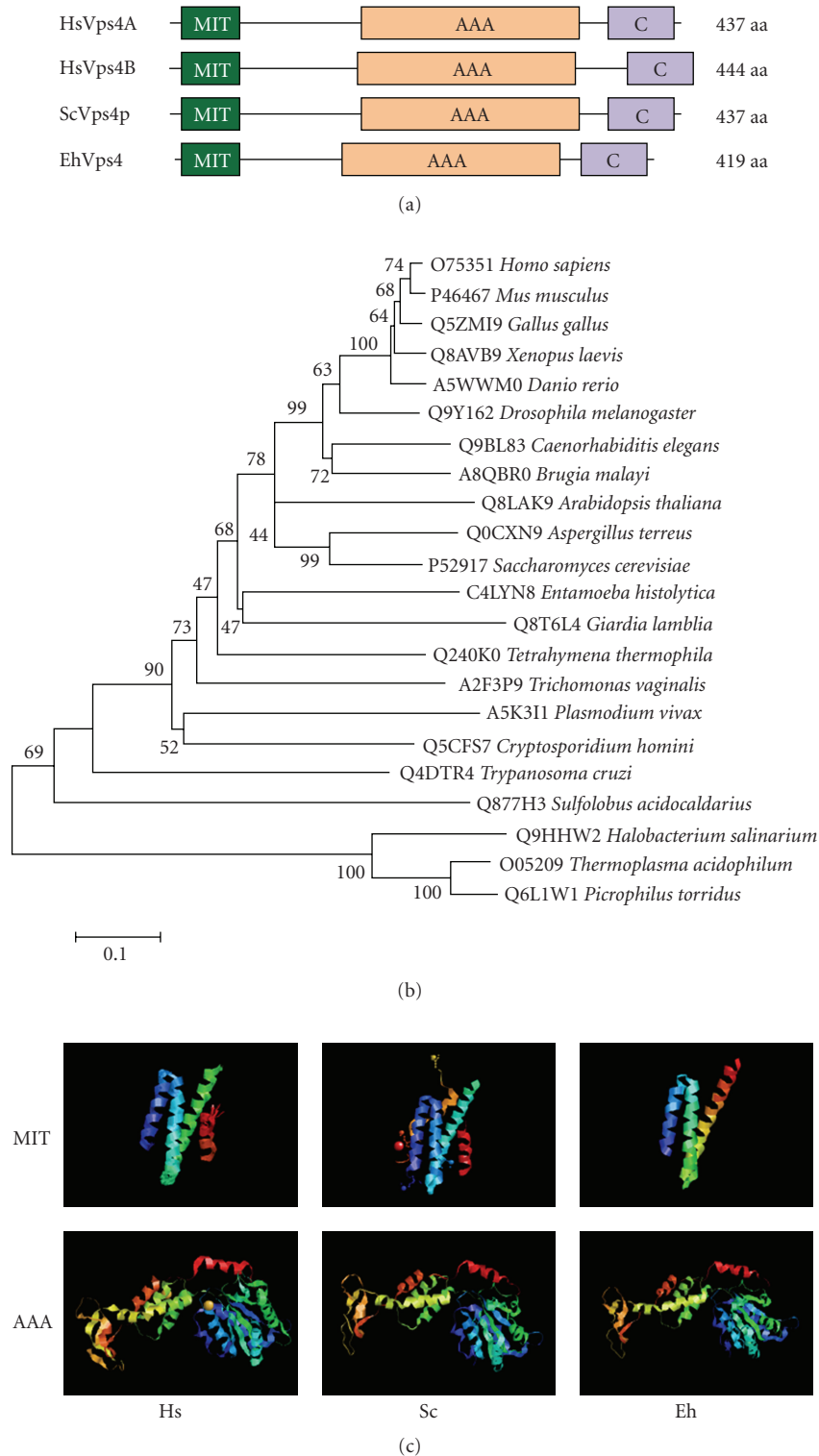
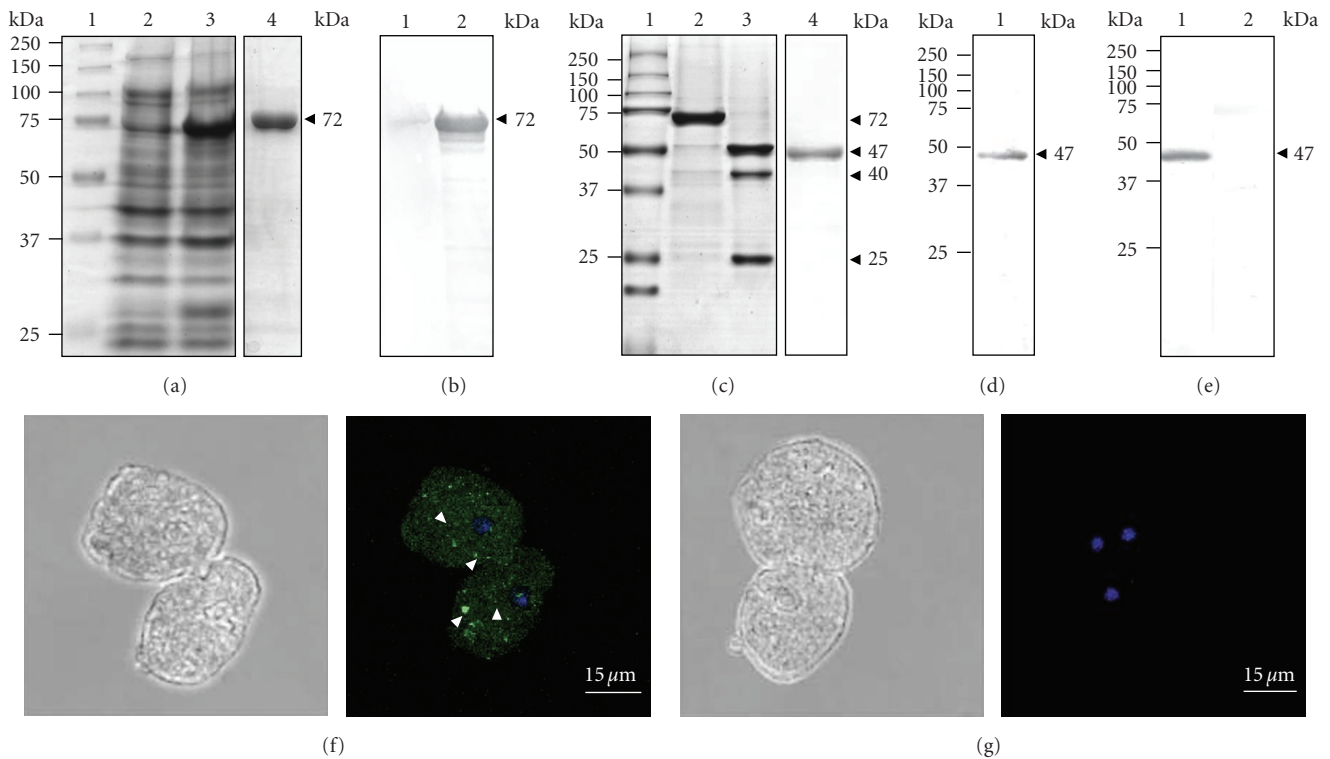


FIGURE 2: Comparison of EhVps4 with other Vps4 proteins. (a) Schematic representation of Vps4 proteins from human, yeast and *E. histolytica*. Conserved MIT, AAA, and Vps4 C-terminal (C) domains were predicted using PROSITE and Pfam programs. (b) Phylogenetic relationships between EhVps4 and homologous proteins from other organisms. The phylogenetic tree of Vps4 homologues was created with the MEGA 3.1 program using the Neighbor Joining algorithm based on ClustalW alignments of complete amino acids sequences. Numbers on tree nodes represent the bootstrap proportions (%) of 1000 replications. The UniProt KnowledgeBase database accession number for each protein is indicated before the organism. (c) Comparison of 3D structures of MIT and AAA domains from human (*Hs*), yeast (*Sc*) and *E. histolytica* (*Eh*) Vps4 homologues. 3D modeling of EhVps4 MIT and AAA domains was obtained using crystal data from yeast Vps4p MIT (2v6xA) and AAA (2qpAB) domains as template, respectively.



**FIGURE 3:** Expression and immunodetection of EhVps4. (a) Expression and purification of recombinant EhVps4-GST polypeptide. Proteins were separated through 10% SDS-PAGE and gels were stained with Coomassie blue. Lane 1, molecular weight markers; lane 2, noninduced bacteria extract; lane 3, IPTG-induced bacteria extract; lane 4, affinity purified rEhVps4-GST from IPTG-induced bacteria extract. (b) Immunodetection of rEhVps4-GST. Western blot assays were performed using noninduced bacteria extract (lane 1) and IPTG-induced bacteria extract (lane 2), with anti-GST antibodies. (c) PreScission Protease digestion of rEhVps4-GST revealed by Coomassie blue stained gels. Lane 1, molecular weight markers; lane 2, purified rEhVps4-GST protein; lane 3, rEhVps4-GST digested with PreScission Protease; lane 4, purified rEhVps4 protein. (d) Immunodetection of purified rEhVps4 protein by Western blot assays using specific anti-rEhVps4 antibodies (lane 1). (e) Immunodetection of EhVps4 in total extracts of trophozoites using specific anti-rEhVps4 antibodies (lane 1) and preimmune serum (lane 2). Proteins are indicated by arrowheads. (f) and (g) Cellular localization of EhVps4 in trophozoites. Trophozoites of clone A were incubated with rabbit anti-rEhVps4 (f) or preimmune (g) serum, treated with FITC-labeled secondary antibodies, counterstained with DAPI and analyzed through confocal laser microscopy. Left, cells observed in phase contrast; right, merge (trophozoites observed in the green (FITC) and blue (DAPI) channels). Arrowheads, EhVps4 signal in small cytoplasmic dots.

proteins in p*EhVps4* and p*EhVps4*-E211Q transfectant cells, whereas no signal was detected in p*NEO* transfectants, as expected (see Figure 5(c), upper panel). However, specific anti-rEhVps4 antibodies recognized endogenous EhVps4 protein in p*NEO* transfectants (see Figure 5(c), middle panel, lane 1), meanwhile signal increased 2.8- and 9.2-fold in p*EhVps4* and p*EhVps4*-E211Q transfectant cells, respectively (see Figure 5(c), middle panel, lanes 2, and 3). Anti-actin antibodies detected similar amounts of protein in the different transfectants (see Figure 5(c), lower panel). For densitometric analysis, actin band was taken as 100% in each lane and used to normalize EhVps4, EhVps4-FLAG, and EhVps4-E211Q-FLAG data (see Figure 5(d)).

**3.6. Cellular Localization of EhVps4-FLAG and EhVps4-E211Q-FLAG Proteins in Transfected Trophozoites.** To investigate the cellular localization of exogenous wild type EhVps4 and mutant EhVps4-E211Q FLAG-tagged proteins in transfected trophozoites, we performed immunofluorescence assays using anti-FLAG antibodies (see Figure 6).

In p*EhVps4* transfected trophozoites, anti-FLAG antibodies detected the overexpressed exogenous protein diffuse in the cytoplasm and at the plasma membrane (see Figure 6(d)). In contrast, in mutant p*EhVps4*-E211Q transfected cells, signal was not observed at the plasma membrane, but it was present as cytoplasmic structures of varying sizes (see Figure 6(f)). As expected, no signal was detected by anti-FLAG antibodies in p*NEO* transfected cells (see Figure 6(b)). Control assays without anti-FLAG primary antibodies did not show any signal in transfected trophozoites (see Figure 6(h)).

**3.7. Cytopathic Activity, Erythrophagocytosis and Liver Abscesses Formation Are Impaired in Trophozoites Overexpressing the Mutant EhVps4-E211Q-FLAG Protein.** To initiate the phenotypical characterization of trophozoites transfected with p*EhVps4* or p*EhVps4*-E211Q constructs, we first evaluated their cytopathic activity and rate of erythrophagocytosis. Nontransfected clone A and p*NEO* transfected cells were used as controls in these experiments. After 1 hour interaction of MDCK cells with trophozoites

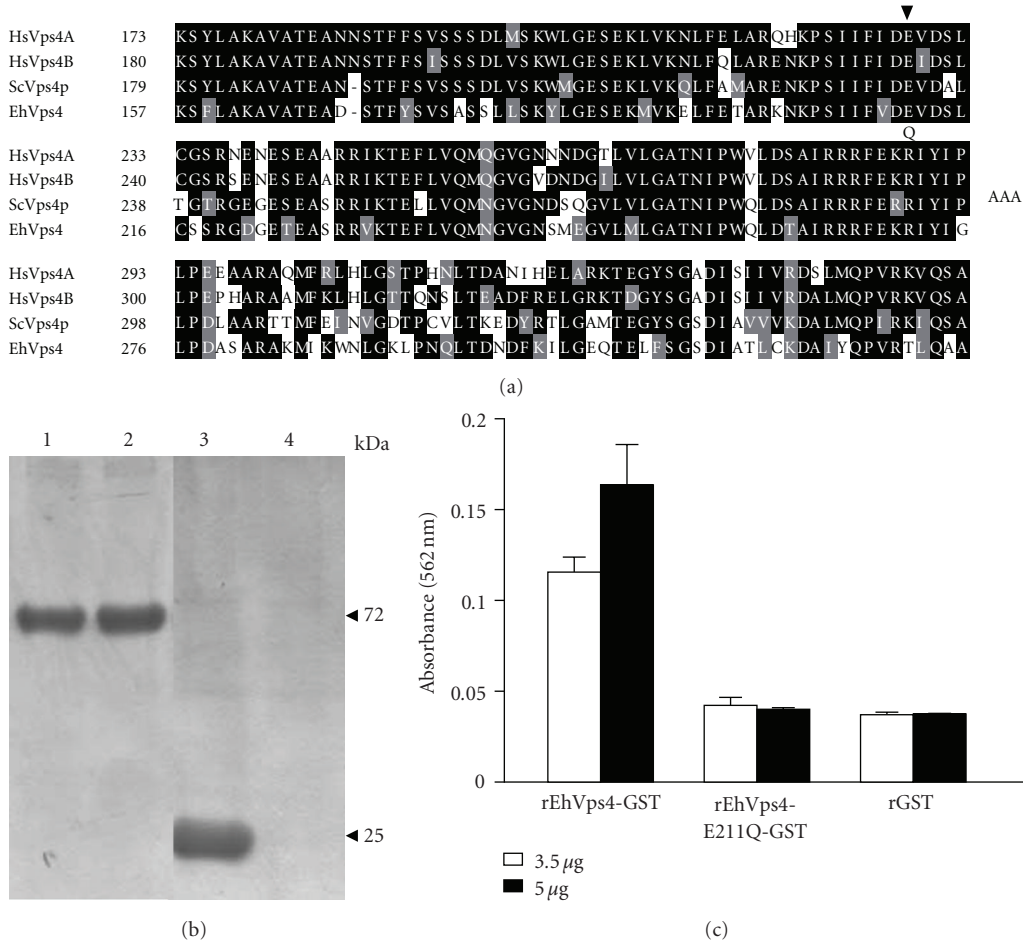


FIGURE 4: Measurement of ATPase activity of recombinant EhVps4. (a) Multiple sequence alignment of Vps4 AAA domain from *Homo sapiens* (HsVps4A and HsVps4B), *S. cerevisiae* (ScVps4p) and *E. histolytica* (EhVps4). Black boxes, identical amino acid (aa); grey boxes, conserved substitutions; open boxes, different aa. Numbers at the left are relative to the position of the initial methionine in each protein. Arrowhead indicates the position of the conserved E residue. (b) Purification of recombinant proteins. Proteins were expressed in *E. coli*, purified through affinity chromatography, separated through 10% SDS-PAGE and stained with Coomassie blue. Lane 1, rEhVps4-GST; lane 2, rEhVps4-E211Q-GST; lane 3, rGST; lane 4, purified fraction from noninduced bacteria extract. (c) ATPase assay. ATPase activity of rEhVps4-GST and rEhVps4-E211Q-GST was monitored as described in Section 2.7. rGST was included as control. Data are the mean of three independent assays.

of clone A, pNEO or pEhVps4 transfected trophozoites, monolayers presented in mean  $86.8 \pm 13.2\%$  destruction. Interestingly, pEhVps4-E211Q transfected cells were less efficient to destroy MDCK cell monolayers, since they only produced  $46.4 \pm 6.4\%$  cell destruction (see Figure 7(a)).

The rates of erythrophagocytosis of non-transfected clone A, pNEO and pEhVps4 transfected cells were similar, at each time tested. In contrast, pEhVps4-E211Q transfected trophozoites showed 60, 55%, and 57% decrease in erythrophagocytosis rate at 5, 10, and 15 minutes, respectively, when compared with the mean rate from the other trophozoites (see Figure 7(b)).

Then, we investigated the capacity of pEhVps4 and pEhVps4-E211Q transfected trophozoites to induce hepatic abscesses formation in hamsters. None of the six hamsters that were infected with pEhVps4-E211Q transfected trophozoites presented hepatic damage (see Figures 7(c)), whereas

the six animals infected with pNEO and pEhVps4 transfected trophozoites developed extensive abscesses.

3.8. EhVps4 Was Detected around Ingested RBC. To determine the localization of EhVps4 in pEhVps4 transfected trophozoites during erythrophagocytosis, we performed immunofluorescence assays with anti-rEhVps4 serum. Antibodies detected EhVps4 as a signal surrounding ingested erythrocytes, suggesting that this protein may be involved in phagocytosis (see Figure 8).

#### 4. Discussion

In *E. histolytica* trophozoites, phagocytosis, and vesicular trafficking are important events for parasite nutrition and destruction of target cells. As in other eukaryotes, the endocytosis and phagocytosis pathways involve the formation of

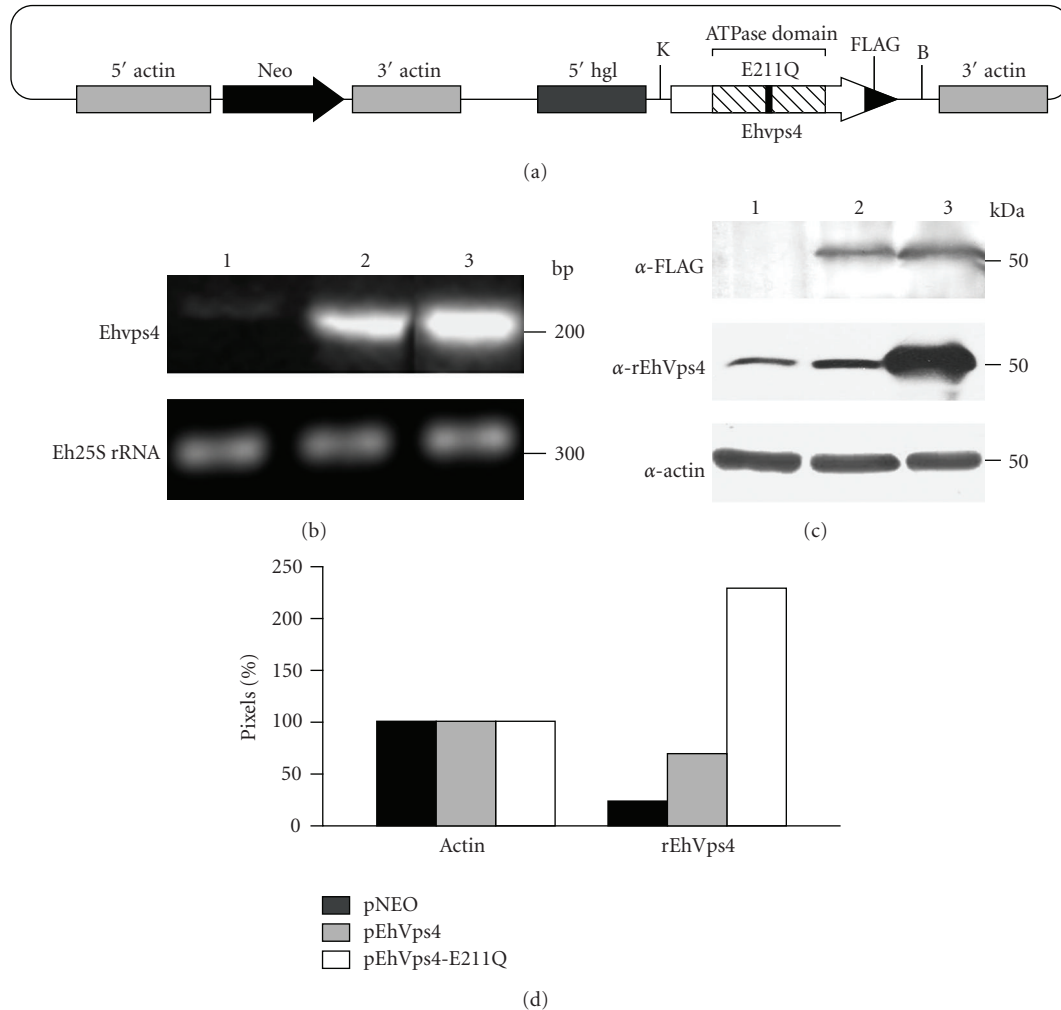


FIGURE 5: Expression of exogenous EhVps4 in transfected trophozoites. (a) Schematic representation of *pEhVps4-E211Q* construct. Mutant *EhVps4* gene was cloned into the *KpnI* and *BamHI* sites of *pNEO* vector, upstream the sequence coding for FLAG epitope. B, *BamHI* site; K, *KpnI* site. (b) 2% agarose gel with RT-PCR assays products. An internal fragment of the *EhVps4* gene (upper panel) or the *Eh25S rRNA* gene (bottom panel) was RT-PCR amplified using 1  $\mu$ g of total RNA from trophozoites of clone A transfected with *pNEO* (lane 1), *pEhVps4* (lane 2) or *pEhVps4-E211Q* (lane 3) plasmid. (c) Western blot assays. Anti-FLAG (upper panel), anti-rEhVps4 (middle panel) and anti-actin (lower panel) antibodies were used to analyze protein lysates (30  $\mu$ g) from *pNEO* (lane 1), *pEhVps4* (lane 2) and *pEhVps4-E211Q* (lane 3) transfected cells. (d) Densitometric analysis of bands corresponding to actin and EhVps4 in (c). Pixels corresponding to actin control were taken as 100% in each lane and used to normalize EhVps4 data.

endosomes, MVB and lysosomes [5, 43]. Indeed, MVBl-like structures have been detected in trophozoites [26, 27] and within isolated phagosomes [24], but proteins participating in their formation have not been identified.

Here, by mining the parasite genome sequence, we demonstrated the presence of 20 genes that encode putative ESCRT machinery components, which could participate in endosomal transport and MVB formation in *E. histolytica*. Most predicted proteins have the conserved functional domains and share high similarity and phylogenetic relationship with homologous proteins from other eukaryotes, strongly suggesting that they have similar functions. RT-PCR assays evidenced that 15 out of 16 ESCRT components tested are transcribed, which is consistent with the activity of endosome formation and vesicle trafficking exhibited

by *E. histolytica* trophozoites (reviewed in [5, 43]). Except for the *Ehadh112* and *EhVps23* genes, transcript amount was not significantly modified after 5 minutes of RBC interaction. Analysis of published *E. histolytica* microarrays data confirmed that most ESCRT genes are transcribed without any significant change under distinct experimental conditions [44, 45]. However, these experiments were not focused on phagocytosis. Additionally, in *Dictyostelium discoideum*, microarrays assays evidenced that expression of most genes involved in intracellular vesicle traffic is not significantly changed during phagocytosis [46]. In mouse macrophages, phagocytosis causes cellular redistribution of Hrs protein (the homologue of yeast Vps27p), but the protein amount remains unchanged [47]. It is possible that trophozoites could have enough ESCRT and associated

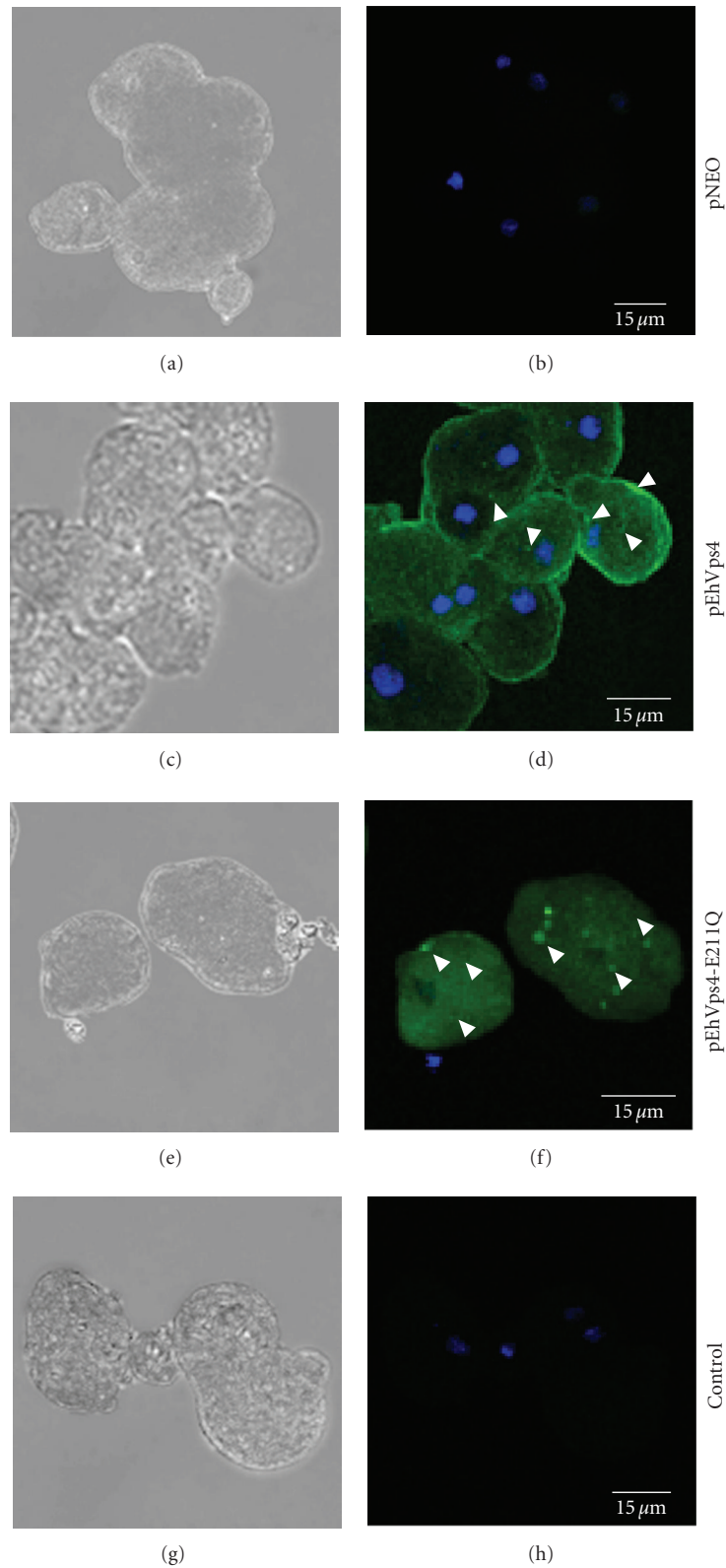


FIGURE 6: Cellular localization of exogenous EhVps4 in transfected trophozoites. Trophozoites transfected with *pNEO* ((a) and (b)), *pEhVps4* ((c) and (d)) and *pEhVps4-E211Q* ((e) and (f)) were incubated with mouse anti-FLAG antibodies, treated with FITC-labeled secondary antibodies, counterstained with DAPI and analyzed through confocal laser microscopy. *pEhVps4-E211Q* transfected trophozoites incubated with FITC-labeled secondary antibodies were used as control ((g) and (h)). (a), (c), (e) and (g) Cells observed in phase contrast; (b), (d), (f) and (h) Merge, trophozoites observed in the green (FITC) and blue (DAPI) channels. Arrowheads, EhVps4 signal in plasma membrane and cytoplasmic dots.

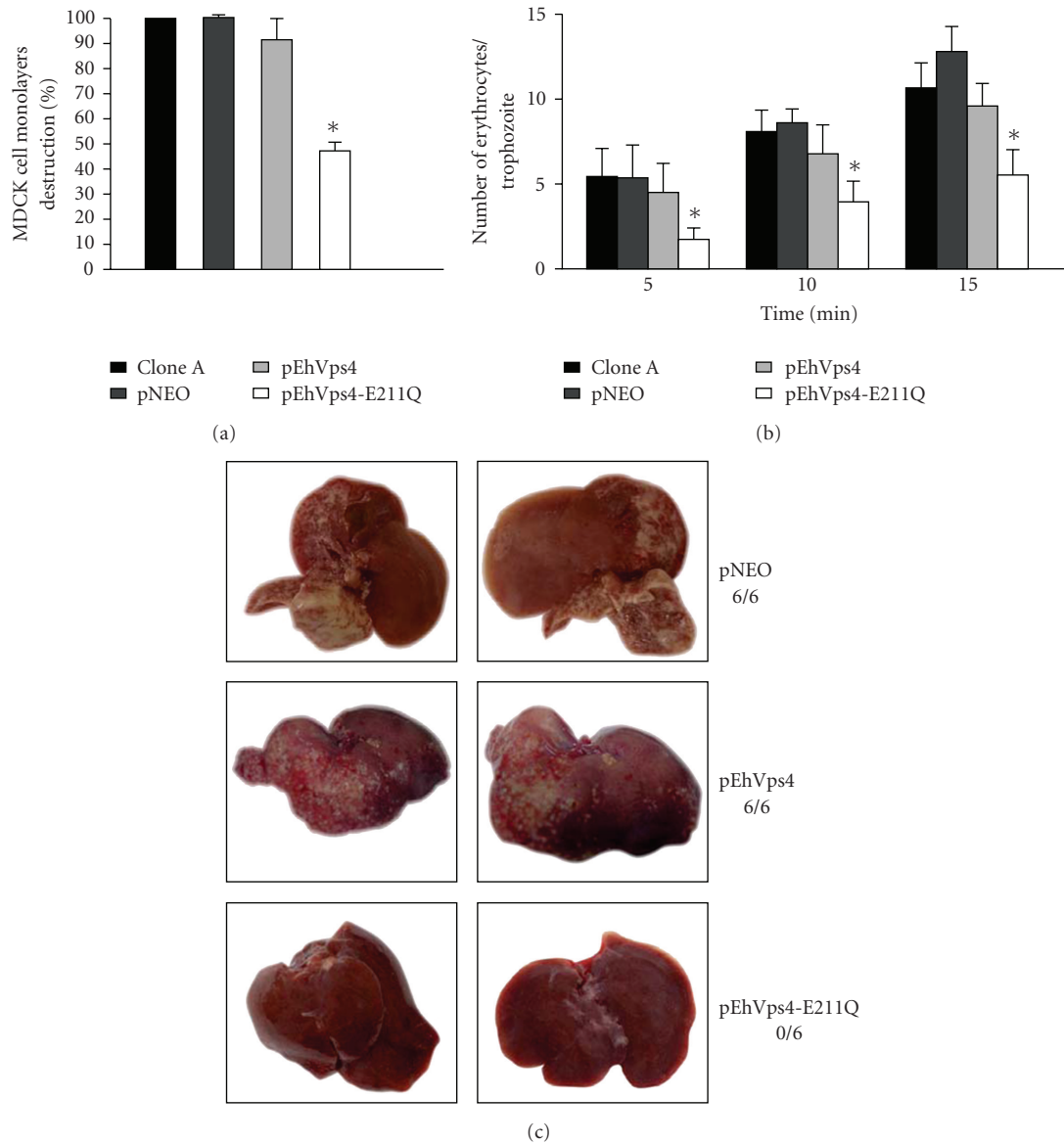


FIGURE 7: Virulence assays of transfected trophozoites. (a) Cytopathic activity. The destruction of MDCK cells monolayers by clone A trophozoites, pNEO, pEhVps4, or pEhVps4-E211Q transfected cells was determined as described [32, 33]. (b) Erythrophagocytosis. Rate of phagocytosis of clone A trophozoites, pEhVps4, pEhVps4-E211Q or pNEO transfected cells was evaluated at 5, 10, and 15 minutes [34]. Histograms show the mean count  $\pm$  SD of three independent experiments by duplicate. (c) Hepatic damage in hamsters infected with transfected trophozoites. Three groups of six hamsters were infected with pNEO, pEhVps4, or pEhVps4-E211Q transfected trophozoites. After 7 days, animals were sacrificed and liver damage was recorded. Pictures were taken from the liver side where the abscesses appeared to be larger and are representative for each group. Upper panels, livers from hamsters infected with pNEO transfected trophozoites (control); middle panels, livers from hamsters infected with pEhVps4 transfected trophozoites; lower panels, livers from hamsters infected with pEhVps4-E211Q transfected trophozoites. 6/6, 6/6 and 0/6 denote number of infected animals/number of inoculated animals.

proteins to perform erythrophagocytosis, if, as we think, these proteins are involved in phagocytosis in *E. histolytica*. However, changes in the gene expression of *E. histolytica* ESCRT members at shorter or larger times cannot be discarded.

In yeast and mammal cells, Vps4 is a key component for disassembly of ESCRT complexes from the endosomal membrane at the MVB invagination pathway [42, 48, 49]. We focused on EhVps4 protein to investigate its role in

endocytosis, specifically in one of the “professional function” of *E. histolytica* trophozoites: phagocytosis. As in yeast, *E. histolytica* has only one *vps4* gene, while higher eukaryotes have two *vps4* genes [21, 50, 51]. By confocal microscopy, EhVps4 was immunodetected as abundant small dots dispersed in the cytosol. In yeast, mammals, plants, and the protozoan *Leishmania major*, similar structures have been identified as MVB formed during endocytosis and vesicular trafficking [22, 42, 51, 52].

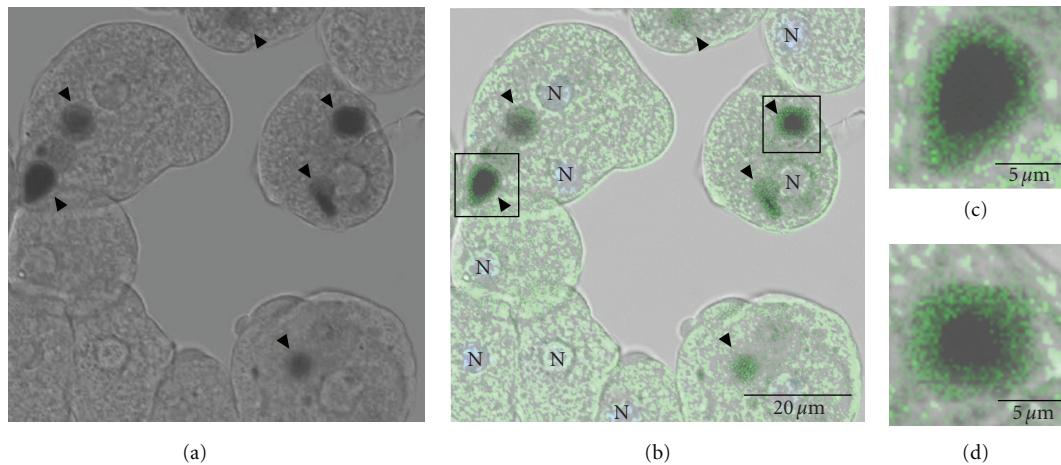


FIGURE 8: Cellular localization of EhVps4 protein during erythrophagocytosis. Trophozoites transfected with p*EhVps4* were incubated with RBC, treated with diaminobenzidine, anti-rEhVps4 and FITC-labeled secondary antibodies, and analyzed through confocal laser microscopy. (a) Cells observed in phase contrast. (b) Trophozoites observed in the green (FITC) channel and phase contrast. (c) Magnification of diaminobenzidine stained RBC squared in (b). Arrowhead, EhVps4 signal around RBC. N, nuclei.

Yeast Vps4p protein exhibits ATPase activity, which depends on the E233 residue present within the AAA domain [18, 42]. In this work, we showed that EhVps4 is an ATPase, which conserves the characteristic domains and folding of Vps4 homologues. This activity depends on the AAA domain since the mutant rEhVps4-E211Q-GST, in which E211 amino acid residue was substituted by Q residue, did not exhibit detectable ATP hydrolysis, as reported in yeast [18, 42].

We further investigated the biological relevance of EhVps4 by generating trophozoites that overexpress wild type EhVps4-FLAG and mutant EhVps4-E211Q-FLAG protein. As the endogenous protein, exogenous EhVps4-FLAG was located in abundant punctuate structures in the cytosol as reported in other organisms [42, 50, 52, 53]. However, overexpressed EhVps4-FLAG was also detected at plasma membrane. In transfected mammal cells that overexpress Sendai virus protein C and wild type Vps4, ALIX/AIP1 proteins are recruited at the plasma membrane to facilitate the budding of virus-like particles [54]. EhADH112, the *E. histolytica* homologue of ALIX, has been detected at the plasma membrane [55]. Experiments currently in progress will help us to define the role of Vps4 at the membrane of trophozoites.

Erythrophagocytosis and cytopathic activities were not improved in trophozoites overexpressing wild type EhVps4-FLAG, probably because other ESCRT proteins are limiting factors for cell destruction and RBC intake [42, 52, 56]. However, the dominant negative effect of mutant EhVps4-E211Q-FLAG protein in MDCK cells destruction, the rate of RBC intake, and liver abscesses formation in hamsters, suggest a role for EhVps4 in *E. histolytica* virulence properties. The localization of EhVps4-FLAG protein around ingested RBC strengthens this hypothesis.

In conclusion, we showed that *E. histolytica* has an ESCRT machinery, which is transcribed in trophozoites. Particularly, we presented evidence that the conserved EhVps4

is an ATPase that could participate in cytopathic activity and erythrophagocytosis, as well as in hepatic damage in hamster. Work currently in progress is focusing on the identification of cytoplasmic structures containing EhVps4, as well as its interaction with other components of the *E. histolytica* ESCRT machinery.

## Acknowledgments

Monoclonal antiactin antibodies were gently provided by Dr. Manuel Hernández (CINVESTAV-IPN). The authors are grateful to M. Sc. Eduardo Carrillo (UACM) for laser confocal microscopy assistance. Their thanks are also to Alfredo Padilla (ICyTDF) for his help in the artwork. This work was supported by a Grant from CONACyT (Mexico) and by CYCYT Grant BFU2005-01970 (to O. Vincent).

## References

- [1] M. D. Abd-Alla, T. F. H. G. Jackson, S. Reddy, and J. I. Ravdin, "Diagnosis of invasive amebiasis by enzyme-linked immunosorbent assay of saliva to detect amebic lectin antigen and anti-lectin immunoglobulin G antibodies," *Journal of Clinical Microbiology*, vol. 38, no. 6, pp. 2344–2347, 2000.
- [2] M. A. Rodríguez, R. M. García-Pérez, G. García-Rivera, et al., "An *Entamoeba histolytica* Rab-like encoding gene and protein: function and cellular location," *Molecular and Biochemical Parasitology*, vol. 108, no. 2, pp. 199–206, 2000.
- [3] S. Marion, C. Laurent, and N. Guillén, "Signalization and cytoskeleton activity through myosin IB during the early steps of phagocytosis in *Entamoeba histolytica*: a proteomic approach," *Cellular Microbiology*, vol. 7, no. 10, pp. 1504–1518, 2005.
- [4] K. Nakada-Tsukui, Y. Saito-Nakano, V. Ali, and T. Nozaki, "A retromerlike complex is a novel Rab7 effector that is involved in the transport of the virulence factor cysteine protease in the enteric protozoan parasite *Entamoeba histolytica*," *Molecular Biology of the Cell*, vol. 16, no. 11, pp. 5294–5303, 2005.

- [5] W. de Souza, C. Sant'Anna, and N. L. Cunha-e-Silva, "Electron microscopy and cytochemistry analysis of the endocytic pathway of pathogenic protozoa," *Progress in Histochemistry and Cytochemistry*, vol. 44, no. 2, pp. 67–124, 2009.
- [6] J. H. Hurley and S. D. Emr, "The ESCRT complexes: structure and mechanism of a membrane-trafficking network," *Annual Review of Biophysics and Biomolecular Structure*, vol. 35, pp. 277–298, 2006.
- [7] R. L. Williams and S. Urbé, "The emerging shape of the ESCRT machinery," *Nature Reviews Molecular Cell Biology*, vol. 8, no. 5, pp. 355–368, 2007.
- [8] T. E. Rusten and H. Stenmark, "How do ESCRT proteins control autophagy?" *Journal of Cell Science*, vol. 122, no. 13, pp. 2179–2183, 2009.
- [9] C. K. Raymond, I. Howald-Stevenson, C. A. Vater, and T. H. Stevens, "Morphological classification of the yeast vacuolar protein sorting mutants: evidence for a prevacuolar compartment in class E vps mutants," *Molecular Biology of the Cell*, vol. 3, no. 12, pp. 1389–1402, 1992.
- [10] T. Wollert, D. Yang, X. Ren, H. H. Lee, Y. J. Im, and J. H. Hurley, "The ESCRT machinery at a glance," *Journal of Cell Science*, vol. 122, no. 13, pp. 2163–2166, 2009.
- [11] D. J. Katzmman, M. Babst, and S. D. Emr, "Ubiquitin-dependent sorting into the multivesicular body pathway requires the function of a conserved endosomal protein sorting complex, ESCRT-I," *Cell*, vol. 106, no. 2, pp. 145–155, 2001.
- [12] M. Curtiss, C. Jones, and M. Babst, "Efficient cargo sorting by ESCRT-I and the subsequent release of ESCRT-I from multivesicular bodies requires the subunit Mvb12," *Molecular Biology of the Cell*, vol. 18, no. 2, pp. 636–645, 2007.
- [13] M. Babst, D. J. Katzmman, W. B. Snyder, B. Wendland, and S. D. Emr, "Endosome-associated complex, ESCRT-II, recruits transport machinery for protein sorting at the multivesicular body," *Developmental Cell*, vol. 3, no. 2, pp. 283–289, 2002.
- [14] M. Babst, D. J. Katzmman, E.J. Estepa-Sabal, T. Meerloo, and S. D. Emr, "ESCRT-III: an endosome-associated heterooligomeric protein complex required for MVB sorting," *Developmental Cell*, vol. 3, no. 2, pp. 271–282, 2002.
- [15] G. Odorizzi, D. J. Katzmman, M. Babst, A. Audhya, and S. D. Emr, "Bro1 is an endosome-associated protein that functions in the MVB pathway in *Saccharomyces cerevisiae*," *Journal of Cell Science*, vol. 116, no. 10, pp. 1893–1903, 2003.
- [16] J. Kim, S. Sitaraman, A. Hierro, B. M. Beach, G. Odorizzi, and J. H. Hurley, "Structural basis for endosomal targeting by the Bro1 domain," *Developmental Cell*, vol. 8, no. 6, pp. 937–947, 2005.
- [17] N. Luhtala and G. Odorizzi, "Bro1 coordinates deubiquitination in the multivesicular body pathway by recruiting Doa4 to endosomes," *The Journal of Cell Biology*, vol. 166, no. 5, pp. 717–729, 2004.
- [18] M. Babst, T. K. Sato, L. M. Banta, and S. D. Emr, "Endosomal transport function in yeast requires a novel AAA-type ATPase, Vps4p," *The EMBO Journal*, vol. 16, no. 8, pp. 1820–1831, 1997.
- [19] P. I. Hanson and S. W. Whiteheart, "AAA+ proteins: have engine, will work," *Nature Reviews Molecular Cell Biology*, vol. 6, no. 7, pp. 519–529, 2005.
- [20] M. Finken-Eigen, R. A. Rohricht, and K. Kohrer, "The VPS4 gene is involved in protein transport out of a yeast prevacuolar endosome-like compartment," *Current Genetics*, vol. 31, no. 6, pp. 469–480, 1997.
- [21] T. Yoshimori, F. Yamagata, A. Yamamoto, et al., "The mouse SKD1, a homologue of yeast Vps4p, is required for normal endosomal trafficking and morphology in mammalian cells," *Molecular Biology of the Cell*, vol. 11, no. 2, pp. 747–763, 2000.
- [22] T. J. Haas, M. K. Sliwinski, D. E. Martínez, et al., "The *Arabidopsis* AAA ATPase SKD1 is involved in multivesicular endosome function and interacts with its positive regulator LYST-INTERACTING PROTEIN5," *The Plant Cell*, vol. 19, no. 4, pp. 1295–1312, 2007.
- [23] M. Okada and T. Nozaki, "New insights into molecular mechanisms of phagocytosis in *Entamoeba histolytica* by proteomic analysis," *Archives of Medical Research*, vol. 37, no. 2, pp. 244–252, 2006.
- [24] M. Okada, C. D. Huston, B. J. Mann, W. A. Petri Jr., K. Kita, and T. Nozaki, "Proteomic analysis of phagocytosis in the enteric protozoan parasite *Entamoeba histolytica*," *Eukaryotic Cell*, vol. 4, no. 4, pp. 827–831, 2005.
- [25] M. Okada, C. D. Huston, M. Oue, et al., "Kinetics and strain variation of phagosome proteins of *Entamoeba histolytica* by proteomic analysis," *Molecular and Biochemical Parasitology*, vol. 145, no. 2, pp. 171–183, 2006.
- [26] C. Bañuelos, I. López-Reyes, G. García-Rivera, A. González-Robles, and E. Orozco, "The presence of a Snf7-like protein strenghtens a role for EhADH in the *Entamoeba histolytica* multivesicular bodies pathway," in *Proceedings of the 5th European Congress on Tropical Medicine and International Health*, M. J. Boeree, Ed., vol. 978, pp. 31–35, Amsterdam, The Netherlands, May 2007, PP-292.
- [27] C. Bañuelos, G. García-Rivera, I. López-Reyes, and E. Orozco, "Functional characterization of EhADH112: an *Entamoeba histolytica* Bro1 domain-containing protein," *Experimental Parasitology*, vol. 110, no. 3, pp. 292–297, 2005.
- [28] N. Saitou and M. Nei, "The neighbor-joining method: a new method for reconstructing phylogenetic trees," *Molecular Biology and Evolution*, vol. 4, no. 4, pp. 406–425, 1987.
- [29] S. Kumar, K. Tamura, and M. Nei, "MEGA3: integrated software for molecular evolutionary genetics analysis and sequence alignment," *Briefings in Bioinformatics*, vol. 5, no. 2, pp. 150–163, 2004.
- [30] L. S. Diamond, D. R. Harlow, and C. C. Cunnick, "A new medium for the axenic cultivation of *Entamoeba histolytica* and other *Entamoeba*," *Transactions of the Royal Society of Tropical Medicine and Hygiene*, vol. 72, no. 4, pp. 431–432, 1978.
- [31] Student, "The probable error of a mean," *Biometrika*, vol. 6, pp. 1–25, 1908.
- [32] Ch. Avila, B. A. Kornilayev, and B. S. J. Blagg, "Development and optimization of a useful assay for determining Hsp90's inherent ATPase activity," *Bioorganic and Medicinal Chemistry*, vol. 14, no. 4, pp. 1134–1142, 2006.
- [33] L. Hamann, R. Nickel, and E. Tannich, "Transfection and continuous expression of heterologous genes in the protozoan parasite *Entamoeba histolytica*," *Proceedings of the National Academy of Sciences of the United States of America*, vol. 92, no. 19, pp. 8975–8979, 1995.
- [34] M.-K. Sung, C. W. Ha, and W.-K. Huh, "A vector system for efficient and economical switching of C-terminal epitope tags in *Saccharomyces cerevisiae*," *Yeast*, vol. 25, no. 4, pp. 301–311, 2008.
- [35] E. Orozco, A. Martínez-Palomo, and R. López-Revilla, "An in vitro model for the quantitative study of the virulence of *Entamoeba histolytica*," *Archivos de Investigación Médica*, vol. 9, supplement 1, pp. 257–260, 1978.
- [36] R. Bracha and D. Mirelman, "Virulence of *Entamoeba histolytica* trophozoites. Effects of bacteria, microaerobic conditions,

- and metronidazole," *The Journal of Experimental Medicine*, vol. 160, no. 2, pp. 353–368, 1984.
- [37] E. Orozco, G. Guarneros, A. Martínez-Palomo, and T. Sánchez, "Entamoeba histolytica. Phagocytosis as a virulence factor," *The Journal of Experimental Medicine*, vol. 158, no. 5, pp. 1511–1521, 1983.
- [38] V. Tsutsumi, R. Mena-López, F. Anaya-Velázquez, and A. Martínez-Palomo, "Cellular bases of experimental amebic liver abscess formation," *American Journal of Pathology*, vol. 117, no. 1, pp. 81–91, 1984.
- [39] J. H. Hurley and D. Yang, "MIT domainia," *Developmental Cell*, vol. 14, no. 1, pp. 6–8, 2008.
- [40] J. Xiao, H. Xia, J. Zhou, et al., "Structural basis of Vta1 function in the multivesicular body sorting pathway," *Developmental Cell*, vol. 14, no. 1, pp. 37–49, 2008.
- [41] B. Loftus, I. Anderson, R. Davies, et al., "The genome of the protist parasite *Entamoeba histolytica*," *Nature*, vol. 433, no. 7028, pp. 865–868, 2005.
- [42] M. Babst, B. Wendland, E. J. Estepa, and S. D. Emr, "The Vps4p AAA ATPase regulates membrane association of a Vps protein complex required for normal endosome function," *The EMBO Journal*, vol. 17, no. 11, pp. 2982–2993, 1998.
- [43] I. Meza and M. Clarke, "Dynamics of endocytic traffic of *Entamoeba histolytica* revealed by confocal microscopy and flow cytometry," *Cell Motility and the Cytoskeleton*, vol. 59, no. 4, pp. 215–226, 2004.
- [44] J. Santi-Rocca, C. Weber, G. Guigon, O. Sismeiro, J.-Y. Coppée, and N. Guillén, "The lysine- and glutamic acid-rich protein KERP1 plays a role in *Entamoeba histolytica* liver abscess pathogenesis," *Cellular Microbiology*, vol. 10, no. 1, pp. 202–217, 2008.
- [45] J. B. Vicente, G. M. Ehrenkaufer, L. M. Saraiva, M. Teixeira, and U. Singh, "*Entamoeba histolytica* modulates a complex repertoire of novel genes in response to oxidative and nitrosative stresses: implications for amebic pathogenesis," *Cellular Microbiology*, vol. 11, no. 1, pp. 51–69, 2009.
- [46] A. Sillo, G. Bloomfield, A. Balest, et al., "Genome-wide transcriptional changes induced by phagocytosis or growth on bacteria in *Dictyostelium*," *BMC Genomics*, vol. 9, article 291, 2008.
- [47] O. V. Vieira, R. E. Harrison, C. C. Scott, et al., "Acquisition of Hrs, an essential component of phagosomal maturation, is impaired by mycobacteria," *Molecular and Cellular Biology*, vol. 24, no. 10, pp. 4593–4604, 2004.
- [48] M. Sachse, G. J. Strous, and J. Klumperman, "ATPase-deficient hVPS4 impairs formation of internal endosomal vesicles and stabilizes bilayered clathrin coats on endosomal vacuoles," *Journal of Cell Science*, vol. 117, no. 9, pp. 1699–1708, 2004.
- [49] N. Bishop and P. Woodman, "ATPase-defective mammalian VPS4 localizes to aberrant endosomes and impairs cholesterol trafficking," *Molecular Biology of the Cell*, vol. 11, no. 1, pp. 227–239, 2000.
- [50] S. Scheuring, R. A. Rohricht, B. Schoning-Burkhardt, et al., "Mammalian cells express two VPS4 proteins both of which are involved in intracellular protein trafficking," *Journal of Molecular Biology*, vol. 312, no. 3, pp. 469–480, 2001.
- [51] A. Beyer, S. Scheuring, S. Muller, A. Mincheva, P. Lichter, and K. Kohrer, "Comparative sequence and expression analyses of four mammalian VPS4 genes," *Gene*, vol. 305, no. 1, pp. 47–59, 2003.
- [52] S. Besteiro, R. A. M. Williams, L. S. Morrison, G. H. Coombs, and J. C. Mottram, "Endosome sorting and autophagy are essential for differentiation and virulence of *Leishmania major*," *The Journal of Biological Chemistry*, vol. 281, no. 16, pp. 11384–11396, 2006.
- [53] M. Yang, I. Coppens, S. Wormsley, P. Baevova, H. C. Hoppe, and K. A. Joiner, "The *Plasmodium falciparum* Vps4 homolog mediates multivesicular body formation," *Journal of Cell Science*, vol. 117, no. 17, pp. 3831–3838, 2004.
- [54] T. Irie, N. Nagata, T. Yoshida, and T. Sakaguchi, "Recruitment of Alix/AIP1 to the plasma membrane by Sendai virus C protein facilitates budding of virus-like particles," *Virology*, vol. 371, no. 1, pp. 108–120, 2008.
- [55] G. García-Rivera, M. A. Rodríguez, R. Ocádiz, et al., "*Entamoeba histolytica*: a novel cysteine protease and an adhesin form the 112 kDa surface protein," *Molecular Microbiology*, vol. 33, no. 3, pp. 556–568, 1999.
- [56] H. Fujita, M. Yamanaka, K. Imamura, et al., "A dominant negative form of the AAA ATPase SKD1/VPS4 impairs membrane trafficking out of endosomal/lysosomal compartments: class E vps phenotype in mammalian cells," *Journal of Cell Science*, vol. 116, no. 2, pp. 401–414, 2003.